Environmental Factors Affecting Tropical Cyclone Power Dissipation

KERRY EMANUEL

Program in Atmospheres, Oceans, and Climate, Massachusetts Institute of Technology, Cambridge, Massachusetts

(Manuscript received 5 July 2006, in final form 4 April 2007)

ABSTRACT

Revised estimates of kinetic energy production by tropical cyclones in the Atlantic and western North Pacific are presented. These show considerable variability on interannual-to-multidecadal time scales. In the Atlantic, variability on time scales of a few years and more is strongly correlated with tropical Atlantic sea surface temperature, while in the western North Pacific, this correlation, while still present, is considerably weaker. Using a combination of basic theory and empirical statistical analysis, it is shown that much of the variability in both ocean basins can be explained by variations in potential intensity, low-level vorticity, and vertical wind shear. Potential intensity variations are in turn factored into components related to variations in net surface radiation, thermodynamic efficiency, and average surface wind speed.

In the Atlantic, potential intensity, low-level vorticity, and vertical wind shear strongly covary and are also highly correlated with sea surface temperature, at least during the period in which reanalysis products are considered reliable. In the Pacific, the three factors are not strongly correlated. The relative contributions of the three factors are quantified, and implications for future trends and variability of tropical cyclone activity are discussed.

1. Introduction

Variations in tropical cyclone activity are potentially among the more important consequences of climate change, whether natural or otherwise. Various metrics have been used to characterize tropical cyclone activity, including annual storm counts, the total duration of storms whose maximum wind speed exceeds a threshold value (Landsea 1993), hurricane categories (Simpson 1974; Webster et al. 2005), and the Accumulated Cyclone Energy (ACE) index (Bell et al. 2000). In terms of human impacts, one is naturally concerned with the number and intensity of landfalling storms, but owing to potential feedbacks of tropical cyclones on climate (Emanuel 2001), there is also interest in basin-integrated quantities, such as ACE. For the purpose of detecting climate signals, such integral measures may be preferable, owing to the much larger amount of information available for storms over their lifetimes compared to at landfall, and to the tendency for random measurement errors and high frequency fluctuations to cancel in the integral. Here we shall focus on the variability of the power dissipation index (PDI), defined by the author (Emanuel 2005) as

$$\mathrm{PDI} \equiv \int_0^{\tau} V_{\max}^3 \, dt, \qquad (1)$$

where $V_{\max}$ is the maximum surface wind at any given time in a storm, and τ is the lifetime of the event. For the purposes of this paper, the PDI is also accumulated over each year.

Annually accumulated integral metrics such as ACE and PDI show striking variations from year to year and on longer time scales (Bell et al. 2000). In the western portion of the North Pacific, ACE is significantly affected by ENSO (Camargo and Sobel 2005). Emanuel (2005) showed that, in the Atlantic, the PDI, when smoothed over several years, is strongly correlated with sea surface temperature in the later summer and early fall in the tropical Atlantic between Africa and the Caribbean, while in the western North Pacific region, the correlation, though significant, is weaker. Figure 1 shows the PDI for both regions, filtered to remove high-frequency fluctuations, as in Emanuel (2005), but extended through 2005 in the North Atlantic and 2004

Corresponding author address: Kerry Emanuel, MIT, 77 Massachusetts Ave., Rm 54-1620, Cambridge, MA 02139.
E-mail: emanuel@texmex.mit.edu

DOI: 10.1175/2007JCLI1571.1

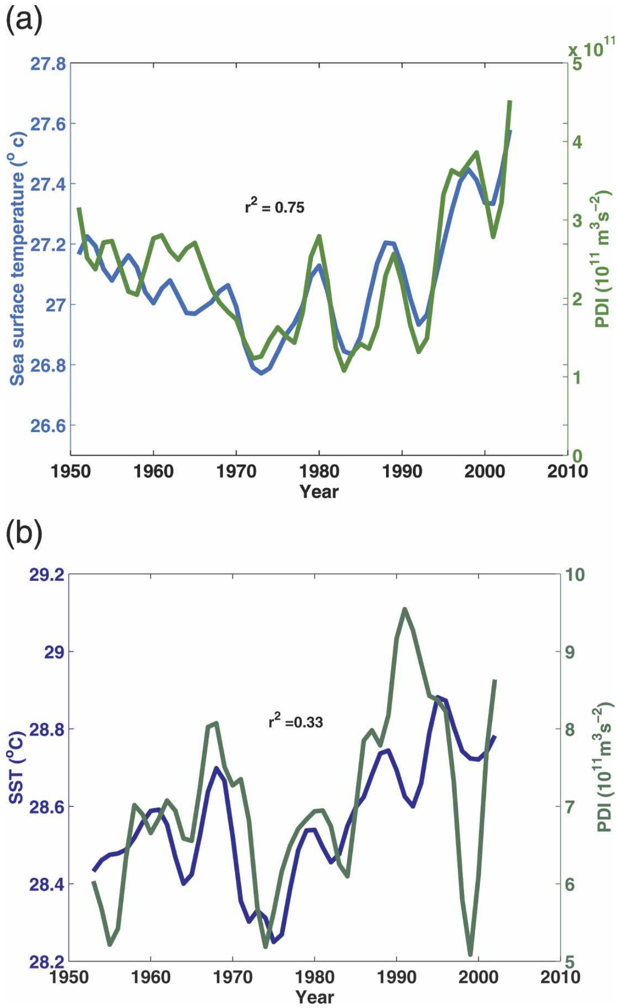

FIG. 1. Power dissipation index (green) and scaled Hadley Centre sea surface temperature (blue) for the main development regions of the (a) Atlantic and (b) western North Pacific. (See text for definitions of regions.) The time series have been smoothed using a 1–3–4–3–1 filter to reduce the effect of interannual variability and highlight fluctuations on time scales of 3 yr and longer.

in the western North Pacific.[1] For comparison, the sea surface temperatures in the main development regions of each basin, as defined in Emanuel (2005), are also shown. In the Atlantic, this is defined as the region bounded by 6° and 18°N and 20° and 60°W, while in the Pacific the development region is defined as being bounded by 5° and 15°N and 130° and 180°E.

As discussed in the online supplement to Emanuel (2005), and in the appendix of this paper, interpretation of the record of tropical cyclone variability is hampered by serious issues of data quality brought about by changing and variable methods of wind speed estimation and reporting problems. On the other hand, the correlations between the smoothed power dissipation and sea surface temperature time series shown in Fig. 1 are both significant at the 99% level and are thus highly unlikely to have arisen by chance elements such as estimation errors.[2]

Since the 1970s, the Atlantic PDI has increased by nearly 100%, while the increase over the same time interval in the western North Pacific has been around 35%. As remarked by Emanuel (2005), these increases are a great deal larger than one might have expected based on extant theory (e.g., Emanuel 1987) and models (Knutson and Tuleya 2004) given the observed changes in sea surface temperature over this period. It should be remarked, however, that these studies considered the response of tropical cyclone intensity (and not frequency or duration) to restricted scenarios of climate change that did not include such factors as changing wind shear or vorticity. In this paper I attempt to resolve this discrepancy by relating the observed changes in PDI to changing environmental factors, using both theoretical and empirical approaches. In the following section, changes in the observed PDI are deconvolved into changing frequency, duration, and intensity. Section 3 reviews and extends existing theory, empirical work, and modeling results as they pertain to PDI, and an attempt is made to apply the results of this work to the development of a semiempirical index relating PDI to three environmental factors. Implications of this work for future changes in PDI are discussed in the concluding section.

2. Contributions to changes in tropical cyclone power dissipation

Annually accumulated PDI may be thought of as depending on the following three factors: storm intensity, duration, and frequency (C. L. Holland and R. B. Scott 2006, personal communication). Because (1) is the sum (over a year) of an integral of the wind speed, there is

[1] There are a plethora of issues surrounding the quality of tropical cyclone data in both basins, and corrections have been made to both datasets. The nature of these issues and the basis of the corrections are described in the appendix. In Fig. 1, we show results using data that have been adjusted as described in the appendix; the reader is also referred to Landsea (2005) for a comparison with the unadjusted data.

[2] The correlation between SST and PDI in the western North Pacific is 0.40 prior to 1983, when JMA data were used, but only 0.01 between 1983 and 2004, when the recent reanalysis by Kossin et al. (2007) was used. (See the appendix.)

no unique way of deconvolving it into factors. Here, we choose to characterize PDI as the product of three factors—the annual number of events N, duration D, and intensity I. The annual number is self-defined. For duration, we could simply choose the average lifetime of a storm, defined as the time between the first and last entries for each event in the tropical cyclone database; this is the approach followed by C. L. Holland and R. B. Scott (2006, personal communication). This definition is perhaps not optimal, because there is often uncertainty in defining when an event first becomes a tropical cyclone and when it ceases to be one, and many storms linger for days at intensities not much above the threshold for classification as a tropical cyclone. To reduce the effect of these pitfalls, we define a velocity-weighted duration of storm i as

$$D_i \equiv \frac{\int_0^\tau V_{\max}\, dt}{V_{\mathrm{smax}}}, \tag{2}$$

where V_{smax} is the maximum wind observed during the lifetime of the storm. Averaging over all storms in a given year yields

$$D = \frac{1}{N}\sum_1^N D_i. \tag{3}$$

Finally, an annually averaged intensity is defined as

$$I = \frac{\sum_{i=1}^{N} \int_0^{\tau_i} V_{\max}^3\, dt}{\sum_{i=1}^{N} D_i}. \tag{4}$$

From (2)–(4), it is evident that the annually accumulated PDI is $N \times D \times I$, from which it follows that $\ln(\mathrm{PDI}) = \ln(N) + \ln(D) + \ln(I)$. Figure 2 shows these terms, with their respective long-term means removed. Each of the terms makes substantial contributions to the observed PDI change. In the Atlantic, the upward trend in PDI since the 1970s is dominated by increasing frequency, but the intensity term has increased by about 60% over that interval, and duration has increased by about 20%. The contributions of the individual factors vary in a complex way in the Pacific. For example, the large net increase in PDI between 1975 and 1990 was dominated by increasing duration and frequency, while the intensity remained constant. Similarly, Camargo and Sobel (2005) found that in the western North Pacific, fluctuations in both duration and intensity contribute to differences in the accumulated cyclone energy, a quantity similar to PDI, between El Niño and La Niña years. In neither basin is there any substantial overall trend in intensity as it has been defined here, but there is substantial variability in intensity and duration over the period of record. Finally, C. L. Holland and R. B. Scott (2006, personal communication) also performed a decomposition of Atlantic hurricanes that is very similar to (2)–(4), except that the duration given by (2) was not weighted by wind speed. They find that between 1970 and 2004 the frequency increased by 71%, while duration and intensity (measured by wind speed cubed) increased by 62% and 44%, respectively. Using instead the definitions given

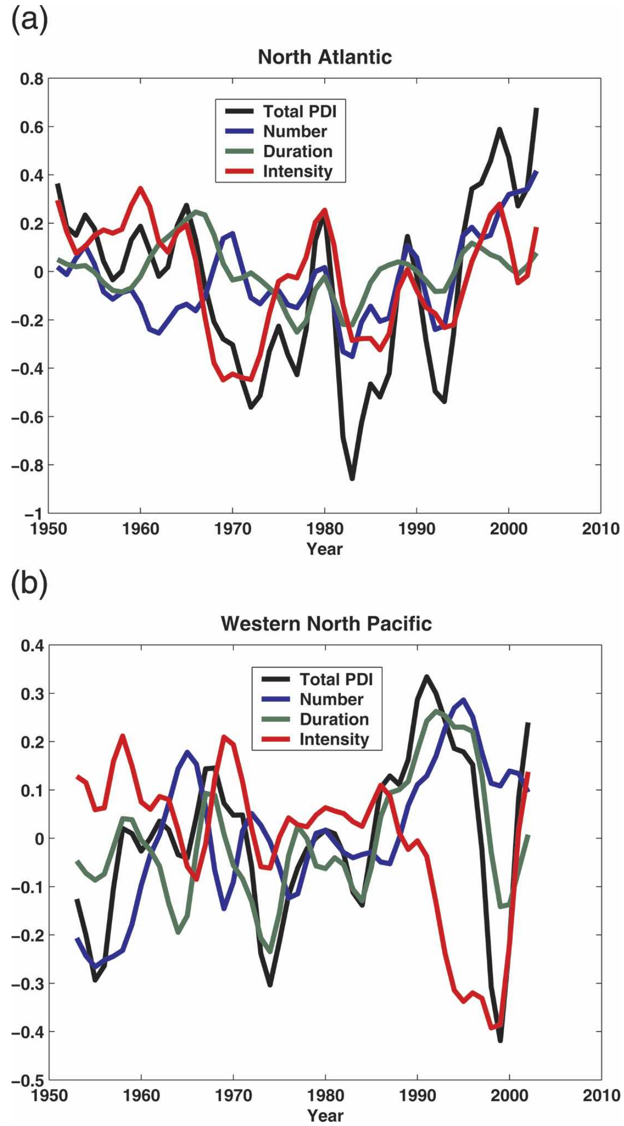

FIG. 2. Deconvolution of the natural logarithm of the power dissipation index (black) into the logarithms of the annual number (blue), duration (green), and intensity (red), for the (a) Atlantic and (b) western North Pacific. The long-term means have been removed, and the time series have been smoothed using a 1–3–4–3–1 filter. Definitions of duration and intensity are given by (3) and (4).

by (2)–(4), for the same period (1970–2004) we find an increase in duration and intensity of 24% and 60%, respectively, showing that the results are sensitive to the way the partitioning is defined.

It should be remarked that the duration, intensity, and annual number of storms are individually not as well correlated with sea surface temperature as is the PDI, suggesting that the latter may be more fundamentally connected with climate variables than traditional metrics. Also, note that our particular decomposition of PDI into frequency, duration, and intensity is sensitive to estimates of the storm lifetime maximum wind speed, which may be prone to sampling error.

In the following section, we review existing theory as well as observational and modeling results as they may bear on the observed PDI variability.

3. Theoretical, modeling, and observational treatment of PDI trends and variability

To understand the observed trends and variability of PDI, it is first necessary to understand environmental controls on tropical cyclone intensity and frequency. We begin with the issue of intensity. Although most empirical studies of the thermodynamic control of tropical cyclone intensity attempt to relate it to sea surface temperature (SST), extant theory suggests that such control is exercised through the potential intensity (Emanuel 1986; Bister and Emanuel 1998), defined as

$$V_p^2 = \frac{C_k}{C_D}\frac{T_s - T_o}{T_o}(k_0^* - k), \tag{5}$$

where V_p is the potential maximum wind speed (hereafter the "potential intensity"), C_k and C_D are the surface exchange coefficients for enthalpy and momentum, respectively, T_s is the sea surface temperature, T_o is an entropy-weighted mean outflow temperature [see Emanuel 1986, his Eq. (19) for an exact definition], k is the specific enthalpy of air near the surface, and k_0^* is the enthalpy of air in contact with the ocean, assumed to be saturated with water vapor at ocean temperature. Modeling studies (Rotunno and Emanuel 1987) suggest that tropical cyclones will attain their potential intensity given long enough to do so, provided that they are unmolested by adverse environmental factors, such as vertical wind shear and ocean interaction.

Few actual storms achieve their potential intensity, and a number of processes have been identified that act to limit storm intensity. Prominent among these is the vertical shear of the environmental horizontal wind (Simpson and Riehl 1958), usually estimated as the magnitude of the vector shear between the lower and upper troposphere (DeMaria 1996), and local cooling of the sea surface as a result of vigorous mixing of the upper ocean (Bender et al. 1993). Ingestion of unusually dry environmental air has also been implicated (Dunion and Velden 2004). An observational analysis (Emanuel 2000) shows that while few real tropical cyclones attain their potential intensity, large samples of their peak intensities, normalized by their potential intensity at the time they achieved their peaks, form a well-defined universal cumulative frequency distribution, suggesting that changing the potential intensity will change the actual mean intensity by the same percentage in a large enough sample of events. In a recent study that used large numbers of modeled storms in environments with realistically varying shear, potential intensity, and upper-ocean conditions, the author Emanuel (2006) found that increasing the potential intensity uniformly by 10% increased the PDI by 65%, while increasing shear by 10% decreased PDI by 12%. Deepening the ocean mixed layer everywhere by 10% increased PDI by 4%. It is important to note that in that study the frequency of events was held constant.

The above suggests that changes in tropical cyclone intensity should be related to changes in potential intensity, shear, upper-ocean temperature profiles, and environmental humidity at midlevels of the troposphere. Evaluating trends in this last quantity would be challenging, owing both to the poor quality of radiosonde humidities at these levels until fairly recently (Spencer and Braswell 1997) and to the problems with the simulation of humidity by models used in reanalysis exercises (Clark and Harwood 2003). The paucity of observations of the tropical upper-ocean makes any analysis of trends in upper-ocean properties highly problematic. For these reasons, we focus on trends in potential intensity and shear.

a. *Environmental control of potential intensity*

According to (5), potential intensity varies with SST, outflow temperature, and the degree of thermodynamic disequilibrium between the ocean and atmosphere. (While the exchange coefficients are known to vary with wind speed, we know of no reason to believe that they vary with climate.) Although the degree of thermodynamic disequilibrium is usually assumed to be a function of SST, its relationship to the state of the ocean–atmosphere system is, in fact, more complex. This can be seen by first considering the steady-state heat balance of the ocean's mixed layer. In equilibrium, the net flux of energy through the sea surface must be balanced by an ocean-side flux of energy into the mixed layer,

$$C_k \rho |\mathbf{V}|(k_0^* - k) + F_\uparrow - F_\downarrow = F_{\text{ocean}}, \tag{6}$$

where ρ is an average air density near the surface, $|\mathbf{V}|$ is the average surface wind speed, $F_\uparrow$ is the net infrared radiative flux out of the ocean, $F_\downarrow$ is the net solar flux into the ocean, and F_{ocean} is the net energy flux into the ocean mixed layer by ocean-side processes, including entrainment. Eliminating the thermodynamic disequilibrium term between (5) and (6) gives

$$V_p^2 = \frac{T_s - T_o}{T_o}\frac{F_\downarrow - F_\uparrow + F_{\text{ocean}}}{C_D\rho|\mathbf{V}|}. \tag{7}$$

This shows that for climate changes on time scales long enough that the ocean's mixed layer remains approximately in thermal equilibrium, the potential intensity is affected by changes in surface and outflow temperatures, radiative flux at the sea surface, mean surface wind speed, and ocean enthalpy fluxes. It is clear from this formulation that in the absence of a greenhouse effect, so that $F_\downarrow = F_\uparrow$, tropical cyclones would not be possible. Also note that in this formulation, the explicit dependence of potential intensity on SST is weak. The strong apparent dependence enters because SST also varies with the surface radiative flux and the surface wind speed. Finally, it is clear from (7) that the sensitivity of potential intensity to radiation is itself modulated by the thermodynamic efficiency [the first factor in (7)] and by the mean surface wind speed.

There are two problems with evaluating changes in potential intensity from historical data. The most straightforward way to is to make use of its equivalence to the convective available potential energy of a parcel lifted from the sea surface after first being saturated with water vapor at sea surface temperature, as described in detail by Bister and Emanuel (2002), who attempted to use reanalysis data (Kalnay et al. 1996) to detect trends. But, this effort is strongly compromised by changes in the types of data assimilated into the reanalysis model, particularly with the introduction of satellite radiance data around 1979, which strongly influenced temperatures in the upper troposphere and lower stratosphere (Santer et al. 1999). The specific effects of this change on potential intensity are also discussed by Free et al. (2004).

Another method is to estimate potential intensity from (7), but this is not usually possible because the net radiative fluxes at the sea surface are not routinely measured. On the other hand, on physical grounds one expects that the surface radiative flux should depend on the profile of temperature and emissivity of the overlying atmosphere. In the Tropics, the temperature profile is usually close to a moist adiabat, whose properties are set mostly by the SST and the near-surface wind speed (Betts and Ridgway 1988), and in the absence of advection, the moisture profile (which largely determines the emissivity) should also vary with these two quantities. For small fluctuations, the relationship should be nearly linear, that is,

$$F_\downarrow - F_\uparrow \simeq a + bT_s + c|\mathbf{V}|, \tag{8}$$

where T_s is in degrees Celsius, $|\mathbf{V}|$ is in meters per second, and a, b, and c are constants. We estimate these constants by regressing (8) so as to best fit the potential intensity determined from National Centers for Environmental Prediction (NCEP) reanalysis data using the method of Bister and Emanuel (2002). As shown in this last-mentioned paper, there are strong, artificial trends in potential intensity estimated this way around 1979, when assimilation of satellite-measured radiances was introduced; to avoid this bias, we fit (8) to (7) using reanalysis data only from 1980 on. We also used the 100-hPa temperature from the NCEP reanalysis as a proxy for the outflow temperature T_o, in (7).[3] This yields $a = -260$ W m^{-2}, $b = 10.3$ W m^{-2} K^{-1}, and $c = 7.8$ W s m^{-3} K^{-1}, a result shown in Fig. 3, which also displays the directly estimated potential intensity. The quantities shown in Fig. 3 have been extended back in time to 1949. To extend the theoretical calculation based on (7) and (8) back in time, one has to account for the large changes in 100-hPa temperature that took place around 1979 owing to the introduction of satellite-derived radiances (Santer et al. 1999; Bister and Emanuel 2002). To do this, we added 3°C to all the 100-hPa temperatures prior to 1979, as suggested by the results of Bister and Emanuel (2002).

The directly calculated potential intensities shown in Fig. 3 have a clear high bias relative to the theoretical predictions prior to 1979, in accordance with the findings of Bister and Emanuel (2002). Figure 3 shows a simple correction to the directly calculated potential intensity, made by subtracting 1.9 m s^{-1} from all the values prior to 1979. This works well in both basins.

It is remarkable that since the 1970s potential intensity has increased by about 10% in the Atlantic and by about 6% in the western North Pacific, given SST changes over the same period of about 0.6° and 0.4°C, respectively. This is considerably more than the change of $\sim$5%°C^{-1} predicted by Emanuel (1987) or the

[3] The outflow level of most tropical cyclones lies between about 200 and 100 hPa. Examination of the basic trends of 150-hPa temperature in the NCEP reanalyses show trends and variability very similar to that at 100 hPa, but with somewhat less cooling between 1990 and 2005. There remains some uncertainty in reanalyzed trends in temperature at these altitudes, owing to changing instrumentation and analysis techniques.

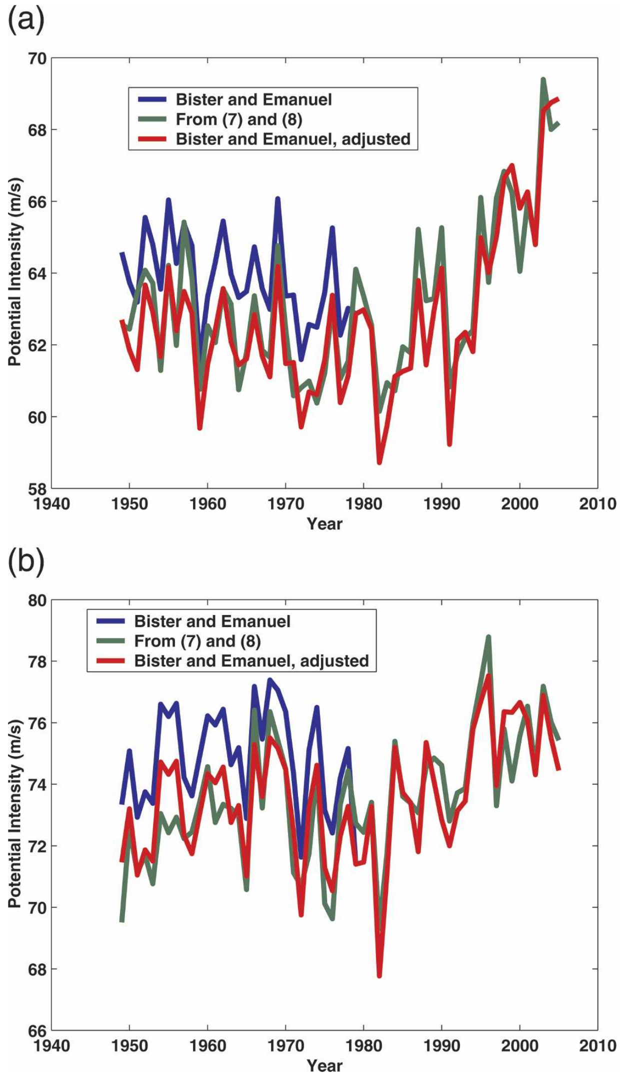

FIG. 3. Evolution of potential intensity in the (a) Atlantic and (b) western North Pacific. The direct calculation from NCEP reanalysis data using the technique of Bister and Emanuel (2002) (blue), theoretical prediction from (7) and (8) (green), and adjusted direct calculation (red) are shown. No smoothing has been applied to the time series.

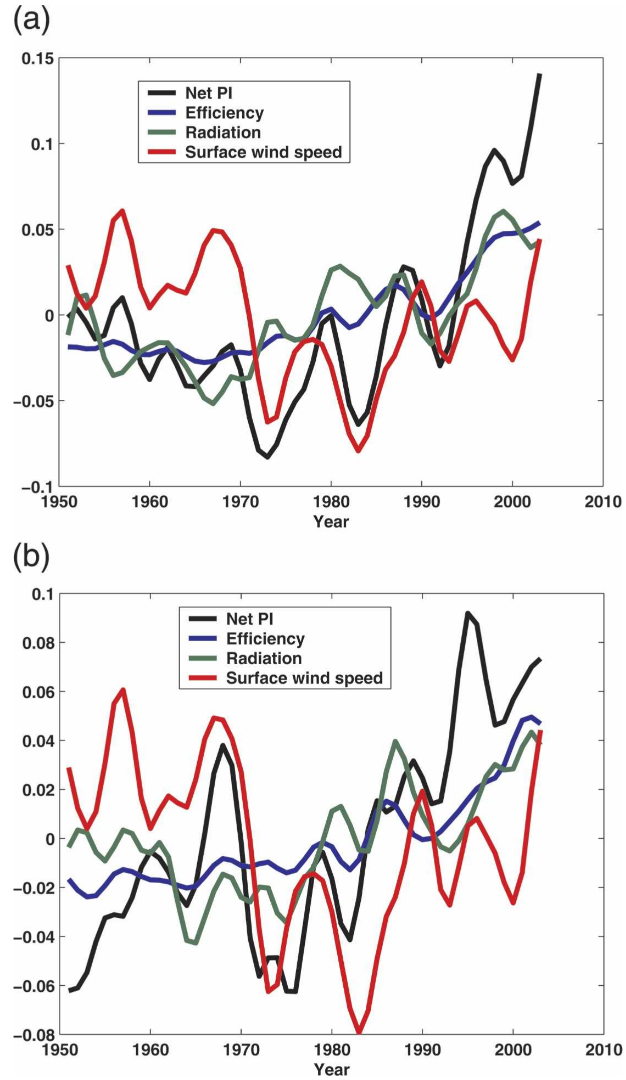

FIG. 4. Deconvolution of the logarithm of the potential intensity given by (7) and (8) (black) into contributions from varying logarithms of the thermodynamic efficiency (blue), surface radiative flux (green), and surface wind speed (red), for the (a) Atlantic and (b) western North Pacific. The long-term means have been removed, and the time series have been smoothed using a 1–3–4–3–1 filter.

$\sim$3.5%$°C^{-1}$ simulated by Knutson and Tuleya (2004). However, differentiating (7) with respect to surface temperature, and using (8), gives a rate of change about 3.2 m s^{-1} K^{-1} for an average V_p of 65 m s^{-1}, and an average surface wind speed of 10 m s^{-1}. (Note that this rate would be about twice as large for a mean surface wind speed of 5 m s^{-1}.) This is well in accord with the aforementioned earlier predictions, and also with what one obtains by differentiating (5) with respect to surface temperature, holding that near-surface relative humidity fixed, and assuming that the surface air temperature equals the sea surface temperature.

To understand the larger observed increases, we separate the potential intensity given by (7) into factors by taking the natural logarithm of both sides of that equation. The three factors are the thermodynamic efficiency $(T_s - T_o)/T_o$, the net surface radiative forcing [as parameterized by (8)], and the surface wind speed. Figure 4 shows variations with the time of the natural logarithm of these factors, with the mean over the period removed. In both basins, all three factors contribute substantially to the overall variability, though the long-term trend is determined by the radiative forcing and thermodynamic efficiency factors. That portion of the variability of potential intensity attributable to fluctuating surface wind speed is remarkably correlated between the two basins. However, wind speed does not contribute to the long-term trend. It is interesting to note that the last points in Figs. 4a,b, representing the smoothed contributions over the 2001–05 period, are contributed to nearly equally by the three factors. It is also of interest to note that the overall upward trend in potential intensity over the last few decades is due to, in nearly equal measure, increasing surface radiative flux and increasing efficiency, the latter of which is owed both to increasing SST and decreasing outflow temperature.

The increase in potential intensity over the past few decades is clearly greater than that predicted to have occurred in conjunction with the observed increase in sea surface temperature according to the theoretical results of Emanuel (1987) or the modeling results of Knutson and Tuleya (2004). The theoretical prediction by Emanuel (1987) held the surface wind speed and thermodynamic efficiency fixed, and thus did not account for these influences on potential intensity; it should also be remarked that the changes in potential intensity presented in that paper that were based on a global climate model simulation also held constant the surface relative humidity and thermodynamic efficiency. The regional model simulations conducted by Knutson and Tuleya (2004) held the surface wind speed fixed, but thermodynamic boundary conditions for those regional simulations were supplied from global climate simulations in which all variables were permitted to change. It is difficult to assess how variable surface wind speed might have indirectly affected the thermodynamic profiles within the regional model domains. Normalized thermodynamic soundings presented by Knutson and Tuleya (2004) show no temperature trend at 100 hPa, but have noticeable cooling above that level.

Thus, much if not all of the discrepancy between the predictions of Emanuel (1987) and observed changes in potential intensity can be ascribed to the effects of changing outflow temperatures and average surface wind speeds in the tropical environment, as remarked previously by the author (Emanuel 2005). It is likely that some, and perhaps most, of the discrepancy between observed changes in potential intensity and those calculated from the model simulations of Knutson and Tuleya (2004) can be similarly ascribed to decreasing outflow temperature and changing environmental surface winds, but it is more difficult to deduce this from the reported results.

It should be remarked that there is only a weak correlation between time series of storm intensity, as it has been defined here (see Fig. 2), and potential intensity, whereas the author (Emanuel 2000) found a strong statistical relationship between peak storm intensity and potential intensity over large samples of events. In that study, the climatological potential intensity at the place and time at which each storm reached its peak intensity was correlated with that intensity; here, the potential intensity is defined over a fixed region, which, while it encompasses the majority of genesis points, is not located in a region where storms often reach their peak intensities.

b. Empirical relationship between power dissipation and environmental factors

While we postulate that potential intensity is the principal thermodynamic factor governing the intensity reached by tropical cyclones, it is well known that other environmental conditions have strong effects on storm intensity and frequency. These include vertical shear of the horizontal wind (DeMaria 1996), ocean interactions (Bender et al. 1993), and environmental relative humidity (Simpson and Riehl 1958; Dunion and Velden 2004). Moreover, genesis frequency appears to be affected not only by potential intensity, vertical shear, and environmental humidity, but also by large-scale, low-level vorticity (Gray 1979; Emanuel and Nolan 2004; Camargo et al. 2007).

We do not have enough observations of upper-ocean profiles over time to make meaningful assessments of the effect of changes in the upper ocean on tropical cyclone power dissipation, so we focus on the effects of variable potential intensity, vertical shear, environmental humidity, and large-scale low-level vorticity. For potential intensity, we use the theoretical values defined by (7) and (8), but as shown by Fig. 3 these are highly correlated with the corrected version of the directly calculated potential intensity. For shear, we use the magnitude of the vector difference of the horizontal wind between 850 and 250 hPa, which appears to be a good predictor of individual storm intensity change (DeMaria and Kaplan 1999). This shear and the other environmental variables are calculated from daily NCEP reanalysis data and averaged over the August–October period in the Atlantic, the July–November period in the western North Pacific, and the respective main development regions, as defined in section 1. It should be remarked that the various predictors should be expected to influence the storm through its whole life, and not just while the storm is within the development regions that we have defined here. Because storms often take very different trajectories, defining sensible regions over which to define the predictors is problematic, and we adhere to the main development regions for no better reason than to maintain continuity with previous studies.

We develop an empirical relationship between year-to-year variations in basin-accumulated PDI and various predictors by selecting candidate predictors and performing multivariate regressions between them and the observed PDI shown in Fig. 1. Because of the aforementioned problems with the reanalysis data, we confine this regression to the period from 1983 to 2005 in the Atlantic, and from 1983 to 2004 in the western North Pacific. In selecting candidate predictors, we are guided by two main considerations. First, in keeping with the inputs required for both the real-time forecasts made using the Coupled Hurricane Intensity Prediction System (Emanuel et al. 2004) and the synthetic storms discussed in the introduction (Emanuel et al. 2006), we take potential intensity V_p and 850–250-hPa shear S as two of our predictors. Second, we make use of additional predictors already shown to be significant in defining a genesis potential index (Emanuel and Nolan 2004; Camargo et al. 2007). These additional predictors are the 850-hPa absolute vorticity η_{850} and the 600-hPa relative humidity. We seek combinations of these parameters that optimally simulate the observed smoothed time evolution of PDI in both basins under consideration here. Both the selection of the predictors and the search for an optimum combination thereof are partially subjective exercises, and we make no representation that we have discovered the optimum combination of predictors. With this important caveat, our PDI predictor is

$$\mathrm{PDI} \sim {\eta_{850}}^{5/2} V_p^7 (1 + 0.3S)^{-4}, \tag{9}$$

where the shear must be given in meters per second. Note that the 600-hPa relative humidity was not found to be a significant predictor of PDI. A comparison between simulated and observed PDI is shown in Fig. 5.

Figure 6 shows the contributions of the logarithm of each of the environmental predictors to changes in the logarithm of the PDI. In the Atlantic, all three quantities contributed roughly equally to variations prior to the late 1980s, but changes since then have been dominated by changing low-level vorticity and potential intensity. In the western North Pacific, the upward trend of potential intensity over the past two decades is largely countered by negative tendencies owing to increasing shear and decreasing vorticity, although there are large swings in these quantities on time scales of 5–10 yr, presumably reflecting the presence of natural climate oscillations (Chan and Shi 1996).

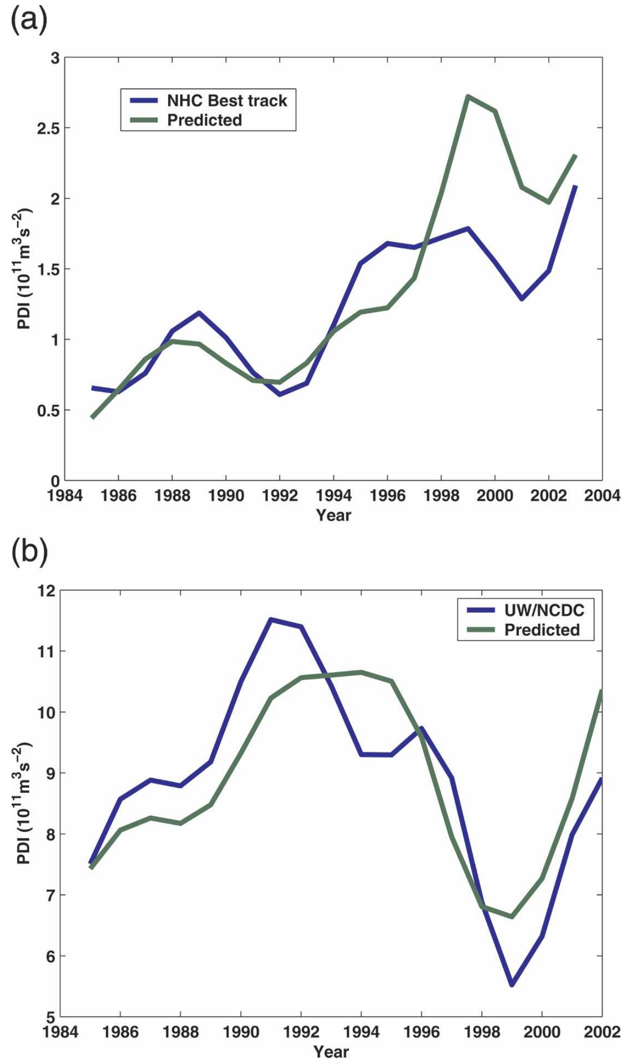

FIG. 5. Evolution of the power dissipation index: observed (blue) and simulated using (9) (green), for the (a) Atlantic and (b) western North Pacific. The time series have been smoothed using a 1–3–4–3–1 filter.

4. Summary

The power dissipation index, a measure of the total energy consumption by tropical cyclones, has been empirically related to a small set of environmental predictors selected on the basis of both theoretical and empirical considerations. The resulting index, given by (9), depends on ambient low-level vorticity, potential intensity, and vertical shear of the horizontal wind. The variability of all three of these factors has contributed significantly to the observed variability of the PDI over the last 25 yr, during which time we have relatively high confidence in both the tropical cyclone record and the reanalysis data. In the Atlantic, the near doubling of the

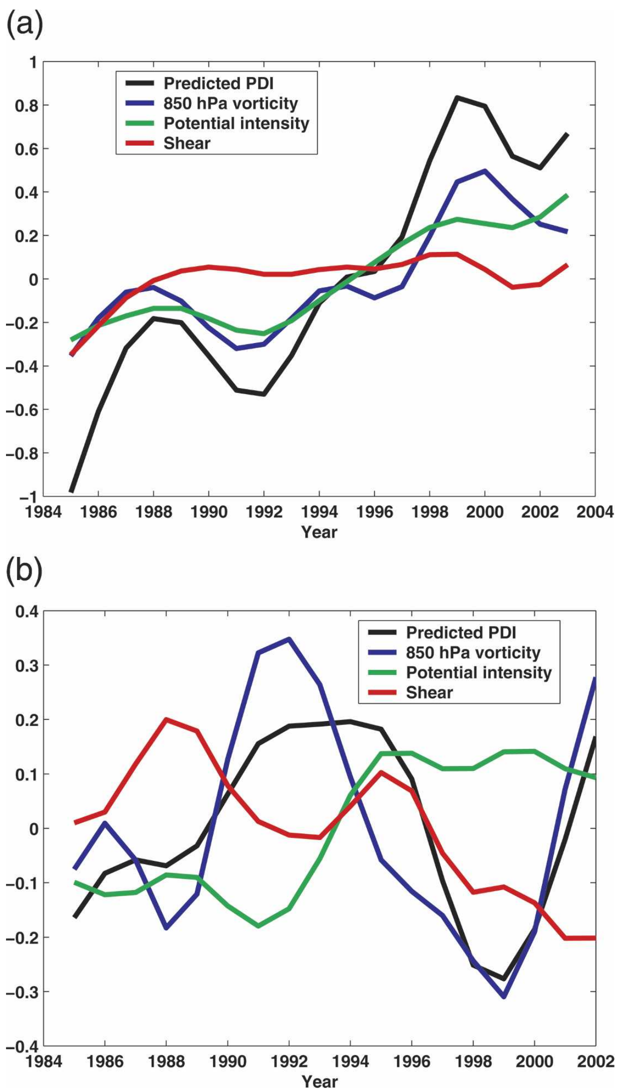

FIG. 6. Deconvolution of the natural logarithm of the power dissipation index given by (9) (black) into contributions from varying natural logarithms of the 850-hPa absolute vorticity (blue), potential intensity (green), and 250–850-hPa wind shear (red), for the (a) Atlantic and (b) western North Pacific. The long-term means have been removed and the time series have been smoothed using a 1–3–4–3–1 filter.

PDI over this period can be attributed to a decrease in shear early in the period and increasing low-level vorticity and potential intensity over the whole period. As shown in Figs. 3 and 4, there has been a ~10% increase in potential intensity in the tropical Atlantic, and a ~6% increase in the western North Pacific during this time, owing mostly to increasing net radiative fluxes into the ocean and decreasing tropopause temperature. Accounting for the influence on the potential intensity of factors other than SST, as well as for the influence of factors other than potential intensity on PDI, largely resolves the discrepancy between observed PDI changes and those predicted on the basis of earlier work.

These results suggest that future changes in PDI will depend on changes not only in surface radiative flux, but in tropopause temperature, surface wind speed, low-level vorticity, and vertical wind shear, as well. These variables are among those simulated by global climate models, which can then be used, in principle, to project future changes in PDI using (9). We are in the process of estimating these changes in the suite of global models being used for the 2007 Intergovernmental Panel on Climate Change (IPCC) report.

Acknowledgments. This research was supported by the National Science Foundation under grant ATM-0349957. This paper profited greatly from thoughtful reviews provided by Chris Landsea, an anonymous reviewer, and an Associate Editor of the *Journal of Climate*, as well as from informal reviews by Judith Curry and Adam Sobel. I thank Jim Kossin for generously providing his new estimates of tropical cyclone wind speed, and helping me correct for missing storms.

APPENDIX

Bias Correction of Tropical Cyclone Wind Speeds

Evolution in measurement and estimation techniques introduces biases in historical records of tropical cyclone wind speeds. These problems are discussed extensively in the online supplement to Emanuel (2005), who also described corrections to the archived data. In the work presented here, we extend that discussion and use two more datasets to refine corrections to the original tropical cyclone data.

Although airborne reconnaissance of tropical cyclones began in the mid-1940s in the both the North Atlantic and western North Pacific, only a relatively small subset of such storms were sampled. In particular, only about half of the Atlantic basin was covered by aircraft reconnaissance in the 1950s and 1960s, and in the absence of satellites, some storms were undoubtedly missed or were poorly sampled; in the western North Pacific, the coverage was worse. In addition, early means of estimating peak wind speeds were primitive, at best. Until the advent of surface-reflecting Doppler radar in the late 1950s, wind speeds were often estimated by visual inspection of the sea surface. However, in a few cases, estimates of central pressure were made by either using dropsondes or integrating the hydrostatic equation down from flight level when radar-derived altitude estimates became available. In these cases, it is possible to estimate wind biases by comparing the wind and pressure estimates, as described presently. The errors that no doubt afflict the earlier data work in both directions; undersampling can lead both to overestimates and underestimates of storm intensity, and estimation errors can also be of either sign.

In the calculation of the Atlantic power dissipation index presented in Emanuel (2005), the author attempted to bias correct the pre-1970 wind records following Landsea (1993). The original correction was presented by Landsea (1993) as a table with seven entries, to which Emanuel (Emanuel 2000) fit a polynomial of the form

$$V' = V[1 - 2 \times 10^{-5}V^2], \tag{A1}$$

where V' is the adjusted velocity and V is the original velocity (both in m s^{-1}). This adjustment is applied to the recorded wind speeds between 1944 and 1969, inclusive. Landsea (2005) points out that his original correction was not intended to increase indefinitely with wind speed. We have therefore developed a new curve fit to Landsea's (1993) correction that tapers to zero at 120 kt, namely,

$$V' = V\left[1 - 0.14\sin\left(\pi\frac{V - 23}{39}\right)\right], \tag{A2}$$

where again V' is the adjusted velocity and V is the original velocity (both in m s^{-1}). This correction is only applied for wind speeds between 23 and 62 m s^{-1}, and only during the years 1944–69, inclusive. We do not correct wind speeds higher than 62 m s^{-1}, because there are not many measurements in these higher ranges and we wish to be conservative in making the adjustment.

The technique for estimating central pressure from reconnaissance aircraft did not change substantially over subsequent years, although the pressure was measured more frequently in later years. Changes in the wind speed–pressure relationship around 1970 motivated Landsea's original corrections. Figure A1a presents a scatterplot of uncorrected winds against central surface pressures for all historical data for which both were available, and for which the central pressure was less than 1000 hPa. The data have been divided into pre- and post-1970 periods. The thick curved lines for each period represent curve fits for the function

$$p_c = 1000\text{hPa} - aV^b, \tag{A3}$$

where the constants a and b are determined by regressing the logarithm of (A3). This is similar in mathematical form to the wind–pressure relationships derived recently by Brown et al. (2006).

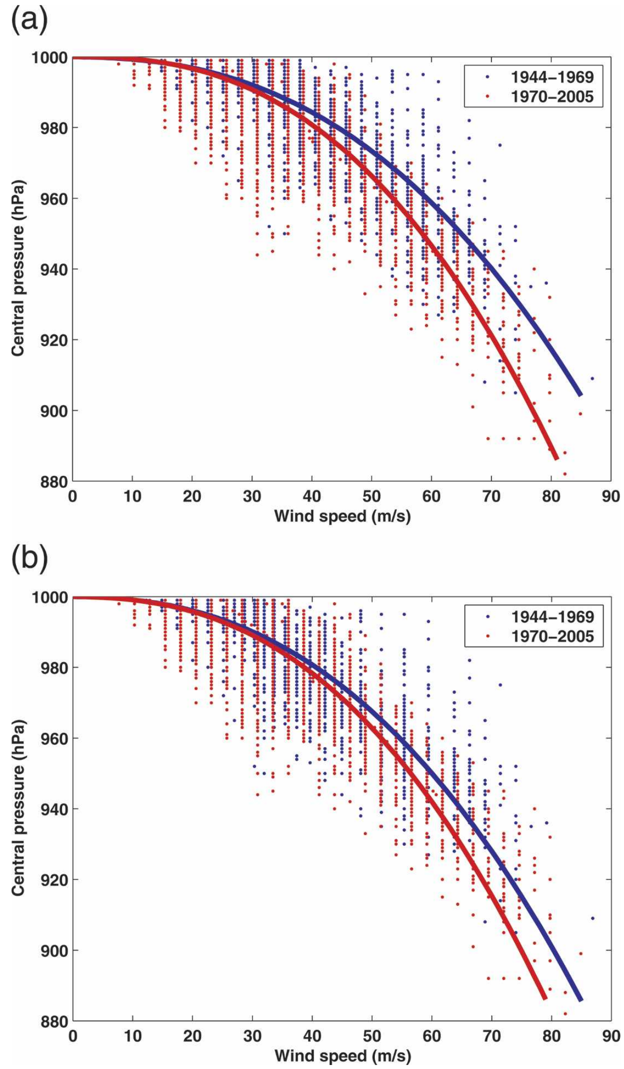

FIG. A1. Scatterplots of observed central pressure vs maximum surface wind speed from the Atlantic best-track data between 1944 and 1969 (blue), and after 1969 (red). (a) The uncorrected data and (b) the corrected winds that have been corrected using (A2) are shown. The curves are best fits of the function given by (A3).

Although there is a great deal of scatter in the wind–pressure relationship in both periods, it is clear from Fig. A1a that winds are generally higher for the same pressure before 1970 compared to after 1970. Figure A1b has the same form as Fig. A1a, but uses the corrected velocities given by (A2) in the pre-1970 period. Judging from the curve fit, the correction given by (A2) is conservative.

The advent of better observations later in the record may also affect estimates of trends in wind speed. There is some indication that wind speeds in the Atlantic in the period from 1970 through the early 1990s may have been underestimated relative to the periods before and

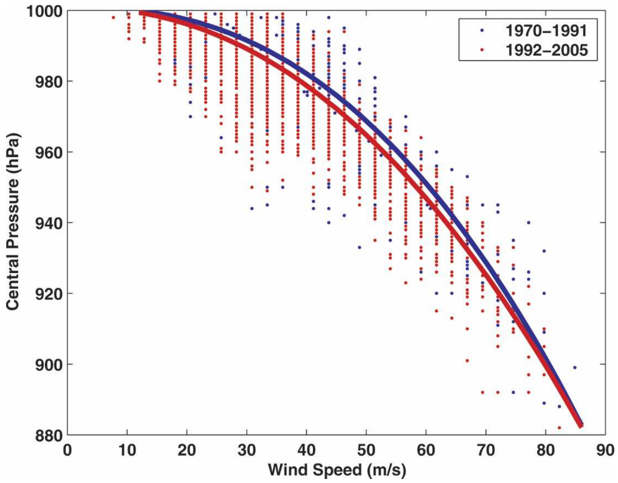

FIG. A2. Scatterplots of observed central pressure vs maximum surface wind speed from the Atlantic best-track data between 1970 and 1991 (blue), and after 1991 (red). The curves are best fits of the function given by (A3).

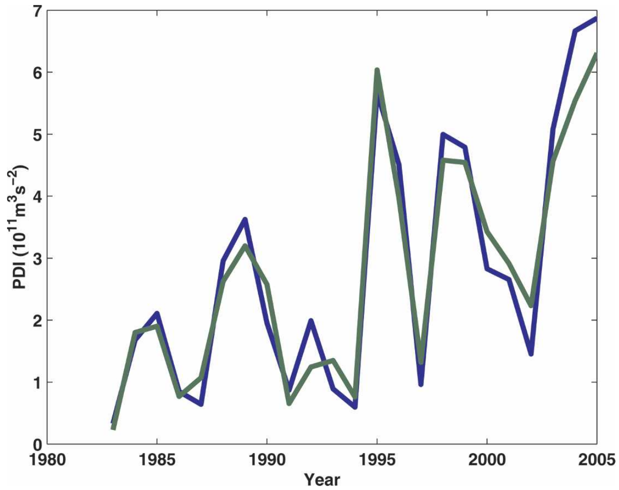

FIG. A3. Time sequence of the (unfiltered) power dissipation index based on unadjusted best-track data (blue) and on the basis of a reanalysis of satellite-based estimates by Kossin et al. (2007) (green), slightly corrected for missing storms as described in the appendix.

after that interval (C. Landsea 2006, personal communication). As a test of this idea, we further subdivided the period 1970–2005 into two subperiods: 1970–91 and 1992–2005. Figure A2 is similar to Fig. A1, but compares these two periods, with curve fits as before. There is a hint that the wind speeds are a little too small in the later period, but the difference is not significant.

Another transition in observing capability took place around 1997, when GPS-based dropsondes capable of superior wind estimates were introduced (Franklin et al. 2003). This led to an upward revision in the relationship used to estimate surface wind speeds given typical flight-level winds. To detect a possible bias arising from this, as well as the aforementioned transition in the early 1990s, we compare the best-track Atlantic data with a new estimate based on a systematic and uniform reanalysis of satellite data (Kossin et al. 2007). The data were obtained from James Kossin, and provide estimates of wind speed every 3 h for most (but not all) Atlantic storms from 1983 to 2005, inclusive. To account for missing storms in this dataset, we calculated the power dissipation index for each year based on this subset of storms, from the original best-track data, and from the full set of storms in the same best-track data. The difference between these two is attributed to the missing storms. We then multiply the power dissipation index based on the new reanalysis data by the ratio of the PDI based on both the full and subset of the best-track data. This correction is small everywhere. Figure A3 compares the evolution of the PDI from the adjusted reanalyzed satellite data to the original best-track data. While there are indeed differences, they are small, and there is no obvious bias change in the early 1990s or around 1997.

Based on this analysis, we use the best-track estimates of PDI with the aforementioned bias adjustment for the years prior to 1970.

In the western North Pacific region, there are yet more serious problems with the tropical cyclone datasets, as discussed in the online supplement to Emanuel (2005). Here we compare the PDI estimated as being bias corrected by Emanuel (2005) to two other estimates. The first of these is the reanalyzed satellite-based estimates of Kossin et al. (2007), corrected for missing storms as described above, and the second is the tropical cyclone archive maintained by the Japanese Meteorological Agency (JMA). In the latter case, we simply take the central pressures reported in the archive and convert them to wind speeds using

$$V = 5.95\sqrt{(1010 - p_c)},$$

where p_c is the reported central pressure (hPa) and V is the maximum wind speed (m s^{-1}). [This is "Takahashi's formula," used by JMA for wind–pressure conversions (K. Kishimoto 2006, personal communication); the JMA data are available online at http://www.jma.go.jp/jma/jma-eng/jma-center/rsmc-hp-pub-eg/besttrack.html.] No corrections of any kind were applied to the JMA data. Figure A4 compares the three estimates of PDI for the western North Pacific. In general the agreement is quite good, with two interesting exceptions. The

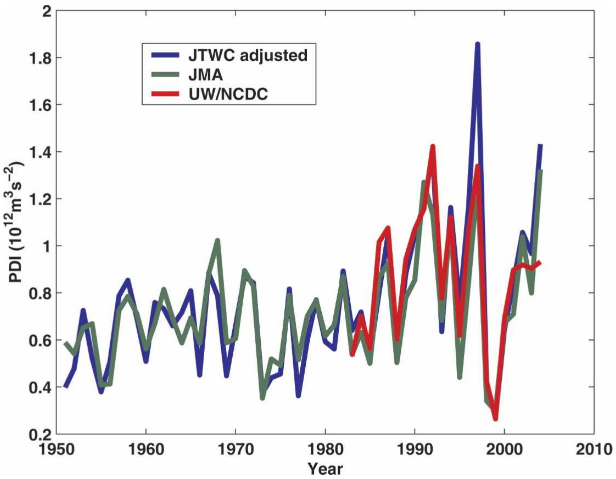

FIG. A4. Time sequence of the (unfiltered) power dissipation index based on JTWC best-track data adjusted as in Emanuel (2005) (blue) on the basis of unadjusted JMA data (green), and a reanalysis of satellite-based estimates by Kossin et al. (2007) (red), slightly corrected for missing storms as described in the appendix.

JTWC data have a large upward spike in 1997, which is much reduced in both the JMA and University of Wisconsin—Madison (UW)/National Climatic Data Center (NCDC) data. Moreover, the large values of PDI in 2005 in the Joint Typhoon Warning Center (JTWC) and JMA datasets are not apparent in the UW/NCDC data. In general, the UW/NCDC reanalysis is in better agreement with the JMA data than with the JTWC data. For this reason, we create a blended dataset, using the UW/NCDC data for the whole period over which it was compiled (1983–2004), and the JMA data from 1951 to 1982, inclusive. All of the discussion and figures in the main body of this paper pertain to this blended dataset. It is interesting to note that the r^2 value between the smoothed SST and smoothed PDI was 0.40 prior to 1983, when the JMA data were used, but only an insignificant 0.01 during the interval 1983–2004, when the Kossin et al. (2007) data were used; these value can be compared to the r^2 value of 0.33 for the blended data extending over the whole period.

Finally, the evaluation of the quality and biases in the wind data by comparison with measured central pressures may be influenced by trends in storm size, storm latitude, and environmental surface pressure, because all three of these factors affect the relationship between maximum wind speed and central pressure, as shown in a recent paper by Knaff and Zehr (2007). Thus, ideally, in correcting winds using central pressure estimates, trends in storm size, latitude, and environmental surface pressure should be accounted for.

REFERENCES

Bell, G. D., and Coauthors, 2000: Climate assessment for 1999. *Bull. Amer. Meteor. Soc.,* **81,** 1328.

Bender, M. A., I. Ginis, and Y. Y. Kurihara, 1993: Numerical simulations of tropical cyclone-ocean interaction with a high-resolution coupled model. *J. Geophys. Res.,* **98,** 23 245–23 263.

Betts, A. K., and W. Ridgway, 1988: Coupling of the radiative, convective, and surface fluxes over the equatorial Pacific. *J. Atmos. Sci.,* **45,** 522–536.

Bister, M., and K. A. Emanuel, 1998: Dissipative heating and hurricane intensity. *Meteor. Atmos. Phys.,* **50,** 233–240.

——, and ——, 2002: Low frequency variability of tropical cyclone potential intensity. 1: Interannual to interdecadel variability. *J. Geophys. Res.,* **107,** 4801, doi:10.1029/2001JD000776.

Brown, D. P., J. L. Franklin, and C. W. Landsea, 2006: A fresh look at tropical cyclone pressure-wind relationships using recent reconnaissance based "best-track" data (1998–2005). Preprints, *27th Conf. on Hurricanes and Tropical Meteorology,* Monterey, CA, Amer. Meteor. Soc., CD-ROM, 3B.5.

Camargo, S. J., and A. H. Sobel, 2005: Western North Pacific tropical cyclone intensity and ENSO. *J. Climate,* **18,** 2996–3006.

——, K. Emanuel, and A. H. Sobel, 2007: Use of a genesis potential index to diagnose ENSO effects on tropical cyclone genesis. *J. Climate,* **20,** 4819–4834.

Chan, J. C. L., and J.-E. Shi, 1996: Long-term trends and interannual variability in tropical cyclone activity over the western North Pacific. *Geophys. Res. Lett.,* **23,** 2765–2767.

Clark, H. L., and R. S. Harwood, 2003: Upper-tropospheric humidity from MLS and ECMWF reanalyses. *Mon. Wea. Rev.,* **131,** 542–555.

DeMaria, M., 1996: The effect of vertical shear on tropical cyclone intensity change. *J. Atmos. Sci.,* **53,** 2076–2087.

——, and J. Kaplan, 1999: An updated Statistical Hurricane Intensity Prediction Scheme (SHIPS) for the Atlantic and eastern North Pacific basins. *Wea. Forecasting,* **14,** 326–337.

Dunion, J. P., and C. S. Velden, 2004: The impact of the Saharan air layer on Atlantic tropical cyclone activity. *Bull. Amer. Meteor. Soc.,* **85,** 353–365.

Emanuel, K. A., 1986: An air-sea interaction theory for tropical cyclones. Part I: Steady-state maintenance. *J. Atmos. Sci.,* **43,** 585–605.

——, 1987: The dependence of hurricane intensity on climate. *Nature,* **326,** 483–485.

——, 2000: A statistical analysis of tropical cyclone intensity. *Mon. Wea. Rev.,* **128,** 1139–1152.

——, 2001: Contribution of tropical cyclones to meridional heat transport by the oceans. *J. Geophys. Res.,* **106,** 14 771–14 782.

——, 2005: Increasing destructiveness of tropical cyclones over the past 30 years. *Nature,* **436,** 686–688.

——, 2006: Climate and tropical cyclone activity: A new model downscaling approach. *J. Climate,* **19,** 4797–4802.

——, and D. Nolan, 2004: Tropical cyclone activity and the global climate system. Preprints, *26th Conf. on Hurricanes and Tropical Meteorology,* Miami, FL, Amer. Meteor. Soc., CD-ROM, 10A.2.

——, C. DesAutels, C. Holloway, and R. Korty, 2004: Environmental control of tropical cyclone intensity. *J. Atmos. Sci.,* **61,** 843–858.

——, S. Ravela, E. Vivant, and C. Risi, 2006: A statistical deterministic approach to hurricane risk assessment. *Bull. Amer. Meteor. Soc.,* **87,** 299–314.

Franklin, J. L., M. L. Black, and K. Valde, 2003: GPS dropwindsonde wind profiles in hurricanes and their operational implications. *Wea. Forecasting,* **18,** 32–44.

Free, M., M. Bister, and K. Emanuel, 2004: Potential intensity of tropical cyclones: Comparison of results from radiosonde and reanalysis data. *J. Climate,* **17,** 1722–1727.

Gray, W. M., 1979: Hurricanes: Their formation, structure, and likely role in the tropical circulation. *Meteorology over the Tropical Oceans,* D. B. Shaw, Ed., Royal Meteorological Society, 155–218.

Kalnay, E., and Coauthors, 1996: The NCEP/NCAR 40-Year Reanalysis Project. *Bull. Amer. Meteor. Soc.,* **77,** 437–471.

Knaff, J. A., and R. M. Zehr, 2007: Reexamination of tropical cyclone wind–pressure relationships. *Wea. Forecasting,* **22,** 71–88.

Knutson, T. R., and R. E. Tuleya, 2004: Impact of CO_2-induced warming on simulated hurricane intensity and precipitation: Sensitivity to the choice of climate model and convective parameterization. *J. Climate,* **17,** 3477–3495.

Kossin, J. P., K. R. Knapp, D. J. Vimont, R. J. Murnane, and B. A. Harper, 2007: A globally consistent reanalysis of hurricane variability and trends. *Geophys. Res. Lett.,* **34,** L04815, doi:10.1029/2006GL028836.

Landsea, C. W., 1993: A climatology of intense (or major) Atlantic hurricanes. *Mon. Wea. Rev.,* **121,** 1703–1713.

——, 2005: Hurricanes and global warming. *Nature,* **438,** E11–E12.

Rotunno, R., and K. A. Emanuel, 1987: An air–sea interaction theory for tropical cyclones. Part II: Evolutionary study using a nonhydrostatic axisymmetric numerical model. *J. Atmos. Sci.,* **44,** 542–561.

Santer, B. D., J. J. Hnilo, T. M. L. Wigley, J. S. Boyle, C. Doutriaux, M. Fiorino, D. E. Parker, and K. E. Taylor, 1999: Uncertainties in observationally based estimates of temperature change in the free atmosphere. *J. Geophys. Res.,* **104,** 6305–6333.

Simpson, R. H., 1974: The hurricane disaster potential scale. *Weatherwise,* **27,** 169–186.

——, and H. Riehl, 1958: Mid-tropospheric ventilation as a constraint on hurricane development and maintenance. *Proc. Technical Conf. on Hurricanes,* Miami Beach, FL, Amer. Meteor. Soc., D4-1–D4-10.

Spencer, R. W., and W. D. Braswell, 1997: How dry is the tropical free troposphere? Implications for global warming theory. *Bull. Amer. Meteor. Soc.,* **78,** 1097–1106.

Webster, P. J., G. J. Holland, J. A. Curry, and H.-R. Chang, 2005: Changes in tropical cyclone number, duration and intensity in a warming environment. *Science,* **309,** 1844–1846.